ARTICLE

Synthesis of Sulfide Solid Electrolytes from Li_2S and P_2S_5 in Anisole

Riku Maniwa,[a] Marcela Calpa,[a,b] Nataly Carolina Rosero-Navarro,[b]* Akira Miura[b]* and Kiyoharu Tadanaga[b]

Received 00th January 20xx,
Accepted 00th January 20xx

DOI: 10.1039/x0xx00000x

We report the liquid-phase synthesis of sulfide solid electrolytes from Li_2S and P_2S_5 using anisole at 200–300 °C under microwave radiation, in which β-Li_3PS_4 and $Li_7P_3S_{11}$ were directly precipitated in anisole in 30 min. Anisole afforded reasonable reactivity toward Li_2S and P_2S_5 to form β-Li_3PS_4 and $Li_7P_3S_{11}$ powders at 200–300 °C. Moreover, a Li_6PS_5Cl precursor solution was synthesized from a Li_3PS_4–anisole suspension by adding ethanol, Li_2S, and LiCl. The proposed synthesis using anisole is advantageous as a simple, short-time process and would be applicable for the production of all-solid-state batteries.

1. Introduction

The development of next-generation Li-ion secondary batteries is desired in various fields, including mobile phones, electric vehicles, and power storage systems.[1–4] One urgent targets for next-generation of Li-ion secondary batteries is to improve their safety. The current Li-ion secondary batteries use organic electrolytes, which involve the risk of leakage and flammability. For this reason, all-solid-state lithium batteries, in which liquid electrolytes are replaced with flame-retardant inorganic solid electrolytes, have drawn considerable attention.

Sulfide solid electrolytes are attractive because of their high ion conductivity, which in some cases is comparable to that in liquid electrolytes.[5–7] In addition, the good ductility of sulfide solid electrolytes is advantageous for producing all-solid-state batteries because the resistance between grain boundaries can be greatly reduced by only cold pressing.[8] Among the sulfide solid electrolytes, Li_2S-P_2S_5 systems with different structures and compositions have been reported with a conductivity ranging between 10^{-6} and 10^{-2} S cm^{-1}.[9–11] For example, α-, β-, and γ-Li_3PS_4 each comprise different arrangement of PS_4^{3-}.[12] $Li_7P_3S_{11}$ is composed of Li^+, PS_4^{3-} and $P_2S_7^{4-}$, and shows a higher ionic conductivity (1.7×10^{-2} S cm^{-1}) than that of β-Li_3PS_4 (3.3×10^{-4} S cm^{-1}).[6,13] In addition to the simple Li_2S-P_2S_5 system, Li_2S-P_2S_5-LiX (X:Cl, Br, I) is a well-known system for producing sulfide electrolytes with a high ionic conductivity (~10^{-3} S cm^{-1}), such as Li_6PS_5X.[14,15]

Liquid-phase synthesis is a promising approach for producing sulfide electrolytes because it has the potential for large-scale synthesis and production of composite electrodes.[16–19] β-Li_3PS_4 and $Li_7P_3S_{11}$ are synthesized in two steps: formation of Li_3PS_4-solvent complexes from Li_2S and P_2S_5 precursors in a solvent; and their decomposition via post heat treatment in an inert atmosphere.[13,20–28] Synthesis of the complexes generally takes more than several hours, and thus a number of studies have focused on shortening the synthesis time of Li_3PS_4-solvent complexes by ultrasonic and microwave irradiations.[24,25,29] Li_6PS_5X halide-containing argyrodite can be synthesized by adding ethanol to dissolve all ion species, followed by heat treatment to remove the ethanol.[29]

In liquid phase synthesis, selection of solvents is a key issue. Synthesis has been reported with solvents such as acetonitrile (ACN), [22,24,25,27,28,30,31] THF[20,25,32,33] and ethyl propionate.[21,29] In the present study, we focused on anisole as a solvent for the synthesis of Li_2S-P_2S_5 based solid electrolytes. There are four reasons for our selection. First, anisole is an aprotic solvent. When protons are present in the solvent, there is a risk of toxic hydrogen sulfide generation through the exchange reaction between Li^+ in Li_2S and H^+ in the solvent. Second, P_2S_5 is easily dissolved in anisole.[34] It can be expected that the reaction will proceed uniformly and quickly in the liquid phase. Third, the electron-donating ability, which can be quantified by the donor number, is suitable for the synthesis reaction. While a donor number of 0, such as toluene, does not advance the reaction for the synthesis of electrolytes, a number of 14 or above, such as acetonitrile and ethanol, decomposes the solid electrolytes.[35] The donor number for anisole is 9,[36] which is suitable for the synthesis reaction without decomposing the synthesized electrolytes.[35] Fourth, anisole is a solvent that dissolves rubber-based binders.[35] A suspension of the electrode composite, in which the binder is dissolved, can be applied. A sheet-type all-solid-state battery with good uniformity can be constructed. Thus, the proposed liquid-phase synthesis will be easy to apply in the future fabrication of electrode composites.

Here, we proposed a new approach to synthesize various sulfide solid electrolytes using anisole and microwave irradiation. By irradiating with microwaves, the suspension of anisole and sulfide electrolytes was directly obtained from Li_2S and P_2S_5 in 30 min.

[a] Graduate School of Chemical Sciences and Engineering, Hokkaido University, Sapporo Hokkaido 060-8628, Japan.
[b] Division of Applied Chemistry, Faculty of Engineering, Hokkaido University, Sapporo Hokkaido 060-8628, Japan.
*E-mail address: amiura@eng.hokudai.ac.jp; rosero@eng.hokudai.ac.jp

2. Experimental

2.1 Synthesis of solid electrolyte

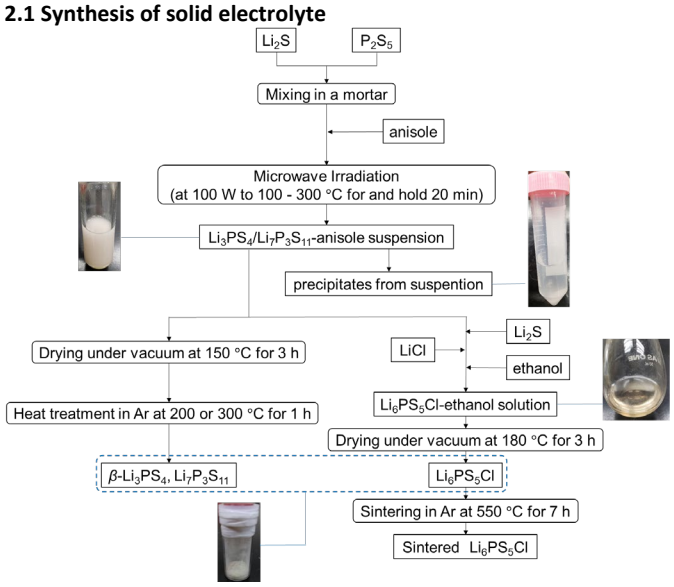

Figure 1. Synthesis process and obtained suspension, solution and powders. Precipitates from suspension, vaccumed powders and sintered Li_6PS_5Cl were characterized.

Figure 1 shows overall synthesis scheme. For the synthesis of β-Li_3PS_4 and $Li_7P_3S_{11}$, the starting materials were Li_2S (Mitsuwa Chemical, 99.9%) and P_2S_5 (Aldrich, 99%), and anisole (Fujifilm Wako Pure Chemical) was used as a solvent. After heating by microwave irradiation, a white suspension was obtained. The suspension was centrifuged, and the obtained precipitates were evaluated. The solid electrolyte powders were obtained by drying under vacuum followed by heat-treatment. For Li_6PS_5Cl, Li_2S, LiCl (Aldrich, 99.9%) and ethanol (Fujifilm Wako Pure Chemical) were added to the suspension, producing transparent solution. This solution was dried under vacuum and powders were sintered. Detailed reagent and solvent amounts are summarized in the supplementary information (Table S1).

2.1.1. Synthesis of β-Li_3PS_4

Anisole was kept in the bottles with molecular sieve to remove water. Pristine Li_2S and pulverized Li_2S by planetary ball milling in a zirconium jar at 500 rpm for 12 hours were used. This ball-milled Li_2S were used only for β-Li_3PS_4 composition after heat treatment in order to examine the effect of the size of Li_2S particle on Li_2S residual (shown in Figure 5). These samples were treated under an Ar atmosphere to avoid moisture.

Powder of Li_2S (Mitsuwa Chemical, 99.9%) and P_2S_5 (Aldrich, 99%) at a molar ratio of Li_2S:P_2S_5=75:25 were mixed in a mortar and pestle. The powders and anisole were placed in a 20 mL borosilicate microwave vial (Anton Paar). Microwave irradiation (2.45 GHz) was applied to the mixture using a microwave reactor (Monowave 400, Anton Paar). The microwave output power was set to 100 W, and an infrared sensor was used to control the temperature. The microwave irradiation was applied until the temperature reached 180-300 °C in 2-7 min (stirring rate was 1200 rpm). Liquid-phase synthesis above the boiling point (anisole:153.8 °C) was performed using a closed vial. After heating to the target temperature, the temperature was maintained for 20 min by adjusting the microwave output. A portion of the suspension was centrifuged, and the precipitates were evaluated. The obtained suspension was dried at 150 °C for 3 h under vacuum to remove the solvent, and the powder was subsequently heat-treated at 200 °C for 1 h.

2.1.2. Synthesis of $Li_7P_3S_{11}$

Powders of Li_2S without ball milling and P_2S_5 at a molar ratio of Li_2S:P_2S_5=70:30 were mixed. The powder and anhydrous anisole were heated to 260 °C by microwave irradiation and dried under vacuum under the same conditions as for β-Li_3PS_4. The powder was heat-treated at 300 °C for 1 h.

2.1.3. Synthesis of argyrodite, Li_6PS_5Cl

Powders of Li_2S without ball milling and P_2S_5 at a molar ratio of Li_2S:P_2S_5=75:25 were mixed. The powder and anhydrous anisole were heated to 220 °C by microwave irradiation under the same conditions as for β-Li_3PS_4. Then, Li_2S, LiCl, and super anhydrous ethanol were mixed into the obtained suspension (total molar ratio Li_2S:P_2S_5:LiCl = 5:1:2). This addition changed the suspension to a transparent solution. The solution was dried at 180 °C for 4 h under vacuum to remove the solvent to produce the sulfide electrolyte powder. A portion of the electrolyte powder was pressed under 360 MPa and sintered at 550 °C for 7 h in a sealed glass tube.

2.2 Characterization

X-ray diffraction (XRD) patterns were measured using an X-ray diffractometer (Miniflex 600, Rigaku). Diffraction data were collected in the 2θ range between 10° and 40° at a step size of 0.02°.

Raman spectra were measured using a Raman spectrometer (XploRA PLUS, Horiba Scientific) to identify structural units of the solid electrolyte samples. The excitation and intensity of the laser beam were 532 nm and 17 mW, respectively. The ionic conductivity of the pelletized samples was evaluated by electrochemical impedance spectroscopy (EIS). The solid electrolyte powders (30 or 80 mg) were pressed under 360 MPa (at room temperature) and two stainless steel (SS) disks were used as the current collectors. EIS was performed using an impedance analyzer (SI 1260, Solartron) in the frequency range of 0.1 Hz to 1 MHz at the amplitude of 10~30 mV.

3. Results and discussion

3.1 Reaction requirements under microwave irradiation

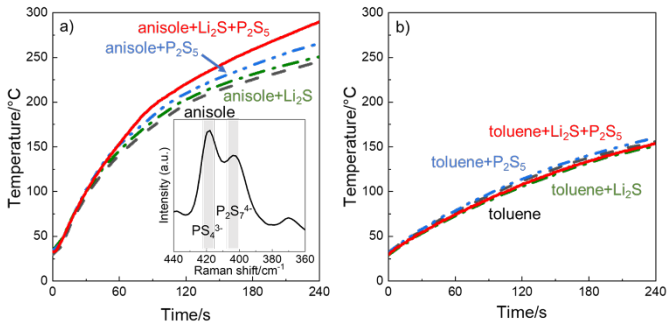

Figure 2. a) The temperature change in anisole during microwave irradiation and Raman spectrum after microwave irradiation (anisole+Li_2S+P_2S_5). b) Temperature change in toluene during microwave irradiation. The microwave output power was 100 W.

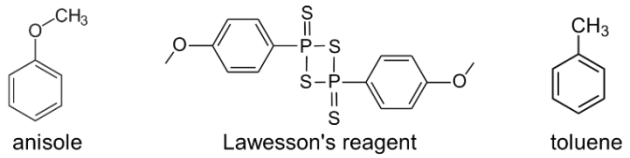

Scheme 1. Structural formulas of anisole, Lawesson's reagent and toluene.

To examine which chemical species absorb microwaves, we investigated the change in temperature of the starting materials under microwave irradiation. Figure 2a shows the temperature change during microwave irradiation. The temperature of all the samples, including anisole without Li_2S and P_2S_5, increased under microwave irradiation, indicating that anisole absorb microwave. While the temperature increase in anisole with Li_2S was comparable to that of anisole alone, the temperature increase in anisole with P_2S_5 was enhanced. Furthermore, the sample with both Li_2S and P_2S_5 in anisole showed the highest temperature. The temperature increase due to microwave irradiation was also confirmed in ACN and THF (Figure S1 a, b), which have been reported as useful solvents in the liquid-phase synthesis of Li_2S-P_2S_5 electrolytes. In contrast, no temperature difference was observed in toluene (Figure 2b). The number of donors in toluene is 0, and the synthesis reaction cannot proceed in toluene.[35] Even though microwave absorption is also affected by the dielectric constant of each solvent, the product of the chemical reaction between Li_2S and P_2S_5 would further absorb microwaves.

The inset of Figure 2a shows the Raman spectra of the precipitate after microwave irradiation of Li_2S and P_2S_5 in the anisole suspension and subsequent centrifugation at 8000 rpm for 10 min. Two Raman bands were centered on 419 and 403 cm^{-1}, attributed to PS_4^{3-} and $P_2S_7^{4-}$ units,[37] and the precipitates were β-Li_3PS_4 or $Li_7P_3S_{11}$, as described in the next section. These ion species can enhance the temperature by Joule heating under microwave irradiation, as suggested earlier. Furthermore, we examined the reactivity between Li_2S and Lawesson's reagents, which has similar components to P_2S_4-anisole (Scheme 1) and is soluble in anisole. In a similar experiment heated at 300 °C, the only product was Li_2S (Figure S2).

To investigate how microwave irradiation affects the products, the same synthesis was performed using a SiC ampule instead of a glass ample. Because the SiC vial absorbs almost all the microwaves to generate Joule heat, the microwave cannot reach inside the sample. Thus, the reactions proceeded only by the thermal effect. Li_2S and P_2S_5 prepared at a molar ratio of 75:25 and anisole as a solvent were added to a 6 mL SiC vial, and microwave irradiation was performed at an output of 100 W for 4 min. No significant difference was observed in the Raman spectra of the products synthesized with glass and SiC (Figure S3). Given that the P-S unit was confirmed, as shown in Figure 2a, it can be seen that Li_2S and P_2S_5 reacted even when a SiC vial was used. Therefore, the reaction of Li_2S and P_2S_5 would dominantly proceed by the thermal effect, and microwave irradiation was effective for quick heating.

3.2 Synthesis of solid electrolytes: suspension and solution

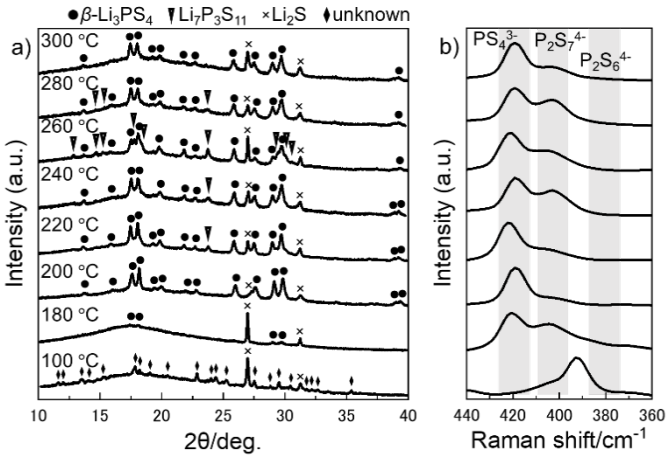

Figure 3. a) XRD pattern and b) Raman spectra of the precipitation (Li_2S:P_2S_5 = 75:25) after microwave irradiation.

Figure 3a shows the XRD patterns of the precipitates obtained by microwave irradiation at different temperatures. The precipitates were collected by centrifugation; thus, no further heat treatment was performed after microwave irradiation. The XRD pattern of the sample heated at 100 °C exhibited peaks assigned to Li_2S as well as additional unknown XRD peaks. The XRD pattern of the sample heated at 180 °C showed Li_2S and β-Li_3PS_4 peaks. The temperature range between 200 and 300 °C showed β-Li_3PS_4 as the main phase, while $Li_7P_3S_{11}$ was detected as a minor phase between 240 and 280 °C. The increase in the ratio of starting materials, Li_2S and P_2S_5, to anisole at heating at 220 °C increased the amount of $Li_7P_3S_{11}$ and Li_2S impurities (Figure S4).

Figure 3b shows the Raman spectra of the obtained precipitates after centrifugation, corresponding to the

conditions shown in Figure 3a. The Raman spectrum of the sample heated at 100 °C exhibited a Raman band centered at 393 cm^{-1}. This band is not attributed to PS_4^{3-} (420 cm^{-1}) or $P_2S_7^{4-}$ (405 cm^{-1}) units.[37] The Raman spectra of all samples heated above 100 °C exhibited a Raman band at approximately 420 cm^{-1}, attributed to PS_4^{3-} units, and an additional band at approximately 405 cm^{-1}, attributed to $P_2S_7^{4-}$ units in the heating temperature range of 240–280 °C.

Unknown peaks in the XRD pattern and the Raman shift to 393 cm^{-1} of the sample heated at 100 °C can be attributed to the complex of Li_3PS_4 and anisole. The formation of β-Li_3PS_4 in the samples heated at temperatures above 100 °C was confirmed by X-ray diffraction and Raman spectroscopy. The intensity of the Raman band attributed to $P_2S_7^{4-}$ units increased at the heating temperature range of 240–280 °C, which explain the additional formation of $Li_7P_3S_{11}$, as observed by X-ray diffraction.

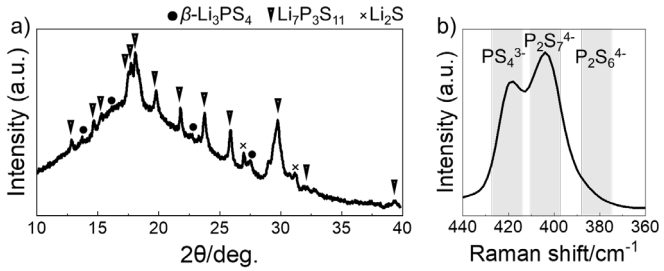

Figure 4. a) XRD pattern and b) Raman spectra of the solid electrolyte (Li_2S:P_2S_5 = 70:30). The suspension was heated at 260 °C by microwave irradiation.

The $Li_7P_3S_{11}$ suspension was synthesized in the same way as for the β-Li_3PS_4 suspension (Figure 3) using a heating temperature of 260 °C and a stoichiometric molar ratio of Li_2S:P_2S_5 = 70:30. Figure 4 shows the XRD pattern and Raman spectrum of the $Li_7P_3S_{11}$ suspension. The XRD pattern (Figure 4a) exhibited the formation of the $Li_7P_3S_{11}$ crystal phase; only minor additional XRD peaks corresponding to Li_2S were observed. The Raman spectrum (Figure 4b) exhibited two main bands at 420 and 405 cm^{-1}, assigned to PS_4^{3-} and $P_2S_7^{4-}$ units.

Figure 5 shows the XRD patterns of the solid electrolytes synthesized from anisole in the present study. After microwave irradiation, the solid electrolytes were dried under vacuum at 150 or 180 °C and subsequently heat-treated at a specific temperature, as described in Figure 1. The synthesized conditions are summarized in Table S1. β-Li_3PS_4 was synthesized from Li_2S with and without ball milling treatment. While ball-milled Li_2S produced single-phase β-Li_3PS_4, Li_2S without ball milling treatment brought about β-Li_3PS_4 with Li_2S impurity. Because ball milling treatment would decrease the particle size of Li_2S, the reaction, smaller particles with larger surface area enhance the reaction between Li_2S and P_2S_5 in anisole. $Li_7P_3S_{11}$ was precipitated as a major phase with a smaller amount of Li_2S. Li_6PS_5Cl was obtained as a single phase and sintering at 550 °C enhanced the crystallinity. Various sulfide solid electrolytes can

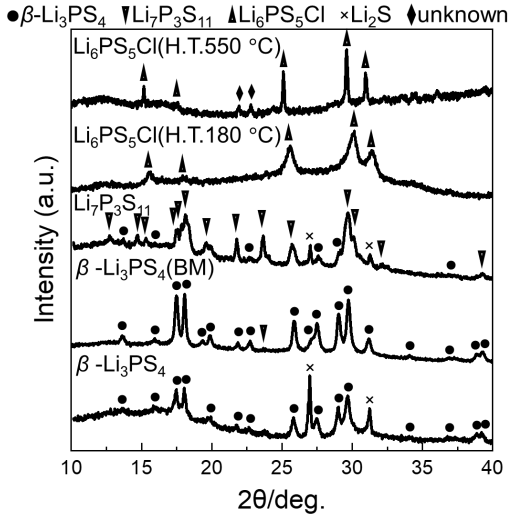

Figure 5. XRD patterns of the solid electrolytes after heat treatment in Ar or vacuum. BM: Ball-milled Li_2S.

be synthesized by a simple process using anisole for liquid-phase synthesis.

Figure 6 shows the Nyquist plots and Table 1 shows the ionic conductivity at room temperature of the prepared solid electrolytes (β-Li_3PS_4, $Li_7P_3S_{11}$, Li_6PS_5Cl). The ionic conductivities heated at 180-300 °C were in the range of 0.05–0.13 mS cm^{-1}. Even though further heat-treatment was necessary, Li_6PS_5Cl pellet heated at 550 °C reached a higher conductivity of 2.1 mS cm^{-1}.[18] . Furthermore, we proved lithium-ion conducting nature of the synthesized $Li_7P_3S_{11}$ electrolyte by discharge-charge properties of the all-solid-state battery with the cathode composite composed of this synthesized $Li_7P_3S_{11}$ (Figure S5)

Compared with previous reports,[20,24,33] the conductivities shown in table 1 tend to be slightly lower. The conductivity may be improved by completely removing any residual water, anisole, and hydrogen in the final product considering that Li_6PS_5Cl electrolyte heated at 550 °C showed one-order higher conductivity than others. A recent work suggests that Li_2S residual which cannot be detected by XRD decreases the ionic conductivity of synthesized electrolytes.[38] Thus, further improvement of the conductivity may be achieved by complete the synthesis reaction.

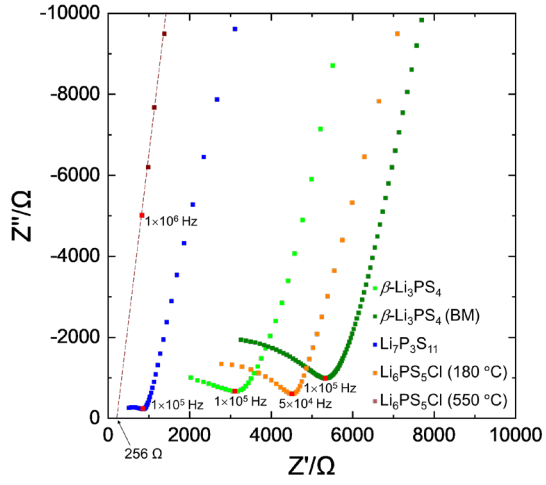

Figure 6. Room-temperature Nyquist plot of the prepared solid electrolyte after heat treatment in Ar or vacuum.

Table 1. Ionic conductivity of synthesized solid electrolyte at room temperature

Product	Microwave/°C	Heat treatment/°C	σ/mS cm^{-1}
β-Li_3PS_4	220	200	0.087
β-Li_3PS_4(BM)	220	200	0.051
$Li_7P_3S_{11}$	260	300	0.13
Li_6PS_5Cl	220	180	0.070
Li_6PS_5Cl	220	550	2.1

As P_2S_5 dissolves in anisole at high temperatures (Figure S6), it is considered that dissolved P_2S_5 is involved in the reaction. In contrast, β-Li_3PS_4 was not obtained from Li_2S and Lawesson's reagent (which can be synthesized from P_2S_5 and anisole) instead of P_2S_5, indicating that the reaction intermediate should not be Lawesson's reagent. Because unreacted Li_2S remained after the reaction to produce β-Li_3PS_4 or $Li_7P_3S_{11}$ under microwave irradiation (Figures 3 and 4), the reaction proceeded from the interface between the dissolved P_2S_5 species (but not Lawesson's reagent) and Li_2S particles. This is supported by enhanced reaction by using ball-milled Li_2S (Figure 5).

In the present study, we synthesized sulfide-based solid electrolytes by taking advantage of anisole with moderate nucleophilic aggression, having a donor number of 9. Although a reaction did not occur in toluene, having a donor number of 0, as a solvent,[35] it is clear that the solvent is involved in the reaction of Li_2S and P_2S_5. The synthesis reaction proceeds in ACN (donor number is 14) to form β-Li_3PS_4 at 200 °C, but further heat treatment above 220 °C resulted in the decomposition of β-Li_3PS_4 electrolytes (Figure S7). Therefore, anisole has the advantage of high-temperature and short-time synthesis, where the reaction kinetics increase without an unfavorable decomposition reaction of β-Li_3PS_4.

4. Conclusions

We succeeded in synthesizing sulfide solid electrolytes, Li_3PS_4, $Li_7P_3S_{11}$, and Li_6PS_5Cl by rapidly heating under microwave irradiation using anisole as a solvent. The advantage of this process is the direct precipitation of solid electrolytes in a solvent, in contrast to other techniques that require a post-heating process to decompose complexes composed of Li_3PS_4 and solvents under an inert atmosphere. Moderate reactivity in anisole allows the synthesis of solid electrolytes at 200–300 °C in a short time. This proposed approach can simplify and shorten the synthesis process, and is promising for producing the components of all-solid-state batteries. These features are advantageous not only for industrial scaling-up but also for producing composite materials with electrode particles and binders. Research on the production of sheet-type batteries using this approach is currently ongoing.

Acknowledgements

This research was partially supported by KAKENHI Grant Number JP19H04682. This work was partially supported by the New Energy and Industrial Technology Development Organization (NEDO), Japan.

References

1 D. Larcher and J. M. Tarascon, *Nat. Chem.*, 2015, **7**, 19–29.
2 B. Dunn, H. Kamath and J.-M. Tarascon, *Science (80-.).*, 2011, **334**, 928–935.A
3 M. Armand and T. and J -M, *Nature*, 2008, **451**, 652–657.
4 M. Li, J. Lu, Z. Chen and K. Amine, *Adv. Mater.*, 2018, **30**, 1–24.
5 N. Kamaya, K. Homma, Y. Yamakawa, M. Hirayama, R. Kanno, M. Yonemura, T. Kamiyama, Y. Kato, S. Hama, K. Kawamoto and A. Mitsui, *Nat. Mater.*, 2011, **10**, 682–686.
6 Y. Seino, T. Ota, K. Takada, A. Hayashi and M. Tatsumisago, *Energy Environ. Sci.*, 2014, **7**, 627–631.
7 Y. Kato, S. Hori, T. Saito, K. Suzuki, M. Hirayama, A. Mitsui, M. Yonemura, H. Iba and R. Kanno, *Nat. Energy*, 2016, **1**, 16030.
8 A. Sakuda, A. Hayashi and M. Tatsumisago, *Sci. Rep.*, 2013, **3**, 2–6.
9 F. Mizuno, A. Hayashi, K. Tadanaga and M. Tatsumisago, *Solid State Ionics*, 2006, **177**, 2721–2725.
10 K. Ohara, A. Mitsui, M. Mori, Y. Onodera, S. Shiotani, Y. Koyama, Y. Orikasa, M. Murakami, K. Shimoda, K. Mori, T. Fukunaga, H. Arai, Y. Uchimoto and Z. Ogumi, *Sci. Rep.*, 2016, **6**, 1–9.
11 A. Hayashi, K. Minami and M. Tatsumisago, *J. Solid State Electrochem.*, 2010, **14**, 1761–1767.
12 K. Homma, M. Yonemura, T. Kobayashi, M. Nagao, M. Hirayama and R. Kanno, *Solid State Ionics*, 2011, **182**, 53–58.
13 N. H. H. Phuc, M. Totani, K. Morikawa, H. Muto and A. Matsuda, *Solid State Ionics*, 2016, **288**, 240–243.
14 S. Boulineau, M. Courty, J. M. Tarascon and V. Viallet, *Solid State Ionics*, 2012, **221**, 1–5.
15 H. J. Deiseroth, S. T. Kong, H. Eckert, J. Vannahme, C. Reiner, T. Zaiß and M. Schlosser, *Angew. Chemie - Int. Ed.*, 2008, **47**, 755–758.
16 S. P. Culver, R. Koerver, W. G. Zeier and J. Janek, *Adv. Energy Mater.*, 2019, **9**, 1–14.
17 A. Sakuda, H. Kitaura, A. Hayashi, K. Tadanaga and M. Tatsumisago, *Electrochem. Solid-State Lett.*, 2008, **11**, 11–14.
18 A. Miura, N. C. Rosero-Navarro, A. Sakuda, K. Tadanaga, N. H. H. Phuc, A. Matsuda, N. Machida, A. Hayashi and M. Tatsumisago, *Nat. Rev. Chem.*, 2019, **3**, 189–198.
19 M. Ghidiu, J. Ruhl, S. P. Culver and W. G. Zeier, *J. Mater. Chem. A*, 2019, **7**, 17735–17753.
20 Z. Liu, W. Fu, E. A. Payzant, X. Yu, Z. Wu, N. J. Dudney, J. Kiggans, K. Hong, A. J. Rondinone and C. Liang, *J. Am. Chem. Soc.*, 2013, **135**, 975–978.
21 N. H. H. Phuc, K. Morikawa, T. Mitsuhiro, H. Muto and A. Matsuda, *Ionics (Kiel).*, 2017, **23**, 2061–2067.
22 R. C. Xu, X. H. Xia, Z. J. Yao, X. L. Wang, C. D. Gu and J. P. Tu, *Electrochim. Acta*, 2016, **219**, 235–240.
23 Y. Wang, D. Lu, M. Bowden, P. Z. El Khoury, K. S. Han, Z. D. Deng, J. Xiao, J. G. Zhang and J. Liu, *Chem. Mater.*, 2018, **30**, 990–997.
24 M. Calpa, N. C. Rosero-Navarro, A. Miura and K. Tadanaga, *RSC Adv.*, 2017, **7**, 46499–46504.
25 K. Suto, P. Bonnick, E. Nagai, K. Niitani, T. S. Arthur and J. Muldoon, *J. Mater. Chem. A*, 2018, **6**, 21261–21265.
26 N. H. H. Phuc, K. Morikawa, M. Totani, H. Muto and A. Matsuda, *Solid State Ionics*, 2016, **285**, 2–5.
27 H. Wang, Z. D. Hood, Y. Xia and C. Liang, *J. Mater. Chem. A*, 2016, **4**, 8091–8096.

28 E. Rangasamy, Z. Liu, M. Gobet, K. Pilar, G. Sahu, W. Zhou, H. Wu, S. Greenbaum and C. Liang, *J. Am. Chem. Soc.*, 2015, **137**, 1384–1387.
29 S. Chida, A. Miura, N. C. Rosero-Navarro, M. Higuchi, N. H. H. Phuc, H. Muto, A. Matsuda and K. Tadanaga, *Ceram. Int.*, 2018, **44**, 742–746.
30 M. Cuisinier, P. E. Cabelguen, B. D. Adams, A. Garsuch, M. Balasubramanian and L. F. Nazar, *Energy Environ. Sci.*, 2014, **7**, 2697–2705.
31 N. C. Rosero-Navarro, A. Miura and K. Tadanaga, *J. Power Sources*, 2018, **396**, 33–40.
32 H. D. Lim, X. Yue, X. Xing, V. Petrova, M. Gonzalez, H. Liu and P. Liu, *J. Mater. Chem. A*, 2018, **6**, 7370–7374.
33 L. Zhou, K. H. Park, X. Sun, F. Lalère, T. Adermann, P. Hartmann and L. F. Nazar, *ACS Energy Lett.*, 2019, **4**, 265–270.
34 I. Thomsen, K. Clausen, S. Scheibye and S.-O. Lawesson, *Org. Synth.*, 1984, **62**, 158.
35 M. Yamamoto, Y. Terauchi, A. Sakuda and M. Takahashi, *Sci. Rep.*, 2018, **8**, 2–11.
36 Y. Marcus, *Chem. Soc. Rev.*, 1993, **22**, 409.
37 F. Mizuno, A. Hayashi, K. Tadanaga and M. Tatsumisago, *Adv. Mater.*, 2005, **17**, 918–921.
38 K. Yamamoto, M. Takahashi, K. Ohara, N. H. H. Phuc, S. Yang, T. Watanabe, T. Uchiyama, A. Sakuda, A. Hayashi, M. Tatsumisago, H. Muto, A. Matsuda and Y. Uchimoto, *ACS Omega*, 2020, **5**, 26287-26294.